
Matrix Phylogeny: Compact Spectral Fingerprints for Trap-Robust Preconditioner Selection

Jinwoo Baek

Department of Computer Science, Oregon State University

Abstract

We introduce *Matrix Phylogeny*, a framework for discovering family-level relationships among matrices via **Compact/Adaptive Spectral Fingerprints** (CSF/ASF). Our fingerprints are low-dimensional, eigendecomposition-free descriptors built from Chebyshev trace moments with Hutchinson sketches, following a simple affine rescaling to $[-1, 1]$ that renders them invariant to permutation and (general) similarity transforms and robust to global scaling.

Across a comprehensive suite (E0–E6+), we observe *phylogenetic compactness*: family identity is captured by only a handful of moments. A fixed small dimension already suffices—**CSF- $K=3-5$** achieves perfect clustering on four synthetic families and a five-family set including BA vs. ER ($ARI=1.0$, silhouettes ≈ 0.89 at $K=3-5$) with the lowest runtimes, while **ASF** adapts on demand (K^* mean 8.4, median 9) serving as a safety net. On a SuiteSparse mini-benchmark with Hutchinson ($p \approx 100$), both CSF-H and ASF-H reproduce the accuracy trend ($ARI=1.0$). Against strong alternatives (eigenvalue histogram + Wasserstein, heat-kernel traces, WL-subtree), CSF- $K=5$ matches or exceeds accuracy while *avoiding* eigendecompositions and using an order-of-magnitude smaller feature dimension (e.g., $K \leq 10$ vs. 64/9153).

The descriptors are stable to noise (log–log slope ≈ 1.03 , $R^2 \approx 0.993$) and enable a practical “trap→recommend” pipeline for automated preconditioner selection. In an adversarial E6+ setting with a Probe-and-Switch mechanism, our physics-guided recommender attains near-oracle iteration counts (regret $p90=0$), whereas a Frobenius 1-NN baseline exhibits large spikes ($p90 \approx 34-60$). Alto-

gether, CSF/ASF provide compact ($K \leq 10$), fast, and invariant fingerprints that unlock scalable, structure-aware search and recommendation over large matrix repositories; we recommend **CSF- $K=5$** by default and **ASF** when domain-specific adaptivity is desired.

1 Introduction

Large matrix repositories arise across simulation, optimization, and machine learning. Practitioners must group matrices by *family resemblance* and make *actionable* choices—e.g., selecting preconditioners—when a new matrix arrives. Entrywise distances ignore spectra; fully spectral methods are costly.

Idea. We propose *Compact/Adaptive Spectral Fingerprints* (CSF/ASF): short descriptors that capture structure without computing eigenvectors or full spectra. After affine rescaling of the spectrum to $[-1, 1]$, we take damped Chebyshev trace moments, yielding invariance to permutation, similarity transforms, and positive scaling. CSF fixes a tiny dimension ($K \in \{3, 5\}$); ASF chooses K via a simple stopping rule. Both support Hutchinson sketches. Pairwise distances induce a dendrogram—*matrix phylogeny*—for retrieval, clustering, and recommendation across heterogeneous sizes.¹

At a glance. Across E0–E6 (synthetics, SuiteSparse, adversarial), a handful of moments identify families: CSF- $K=3-5$ attains $ARI=1.0$ on four synthetic families and on a five-family set including BA vs. ER (silhouette ≈ 0.89) at the lowest runtimes; ASF adapts conservatively (K^* mean 8.4, median 9). On SuiteSparse with Hutchinson ($p \approx 100$), CSF-H/ASF-H match this trend ($ARI=1.0$). Against strong alternatives (eigenvalue histograms + Wasserstein, heat-kernel traces,

¹By “eigendecomposition-free” we mean we never compute eigenvectors nor spectral histograms. For spectrum scaling we may compute scalar endpoints; on small dense cases our prototype obtains them via eigenvalue routines (no eigenvectors), while large runs can rely on matvec-only bounds (power/Lanczos or Gershgorin). Fingerprints are computed via matvec Chebyshev recurrences.

WL-subtree), CSF- $K=5$ matches or exceeds accuracy while using far fewer features ($K \leq 10$ vs. 64/9153) and avoiding full spectra. Fingerprints are noise-stable (slope ≈ 1.03 , $R^2 \approx 0.993$). In adversarial E6+, a *Probe-and-Switch* recommender guided by phylogenetic neighbors attains near-oracle iterations (regret $p_{90}=0$), whereas a Frobenius 1-NN baseline shows large spikes ($p_{90} \approx 34-60$).

Contributions.

- **Framework:** A practical pipeline for *matrix phylogeny* via CSF/ASF that works across sizes without eigenvectors/full spectra.
- **Guarantees:** Invariance, Hutchinson concentration, noise stability, and adaptive stopping (formal statements in the appendix).
- **Evidence:** Strong accuracy at tiny dimensions, matching or exceeding spectral baselines that require full spectra.
- **Actionability:** A robust *Probe-and-Switch* preconditioner selector with near-oracle iterations in adversarial settings.

Organization. Section 3 details the method; Section 4 states guarantees; Section 5 reports E0–E6; we conclude with limitations and related work.

2 Preliminaries

Notation. For $A \in \mathbb{R}^{n \times n}$, let $\lambda_i(A)$ be eigenvalues, $\rho(A) = \max_i |\lambda_i(A)|$ the spectral radius, and $\text{tr}(\cdot)$ the trace. For a polynomial p , $p(A)$ is the matrix polynomial.

Similarity-invariant spectral normalization. We compute fingerprints on \tilde{A} with spectrum in $[-1, 1]$:

$$\begin{aligned} \tilde{A} &= \frac{A - mI}{r}, \quad m = \frac{1}{2}(\lambda_{\max} + \lambda_{\min}), \\ r_0 &= \frac{1}{2}(\lambda_{\max} - \lambda_{\min}), \\ r &= (1 + \varepsilon_{\text{rel}}) r_0 \quad (\varepsilon_{\text{rel}} > 0). \end{aligned} \quad (1)$$

For markedly non-Hermitian inputs we use radius scaling $\tilde{A} = A / \max(\rho(A), \varepsilon_{\text{rad}})$ with tiny $\varepsilon_{\text{rad}} > 0$. In practice, endpoints or $\rho(A)$ come from cheap bounds or a few power/Lanczos steps (Appendix B). Since the normalization depends only on spectral quantities and T_k is a polynomial, $\text{tr}(T_k(\tilde{A}))$ is invariant to permutations, similarities $S^{-1}AS$, and positive scalings αA .

Eigendecomposition-free Chebyshev moments. With $T_0(x) = 1$, $T_1(x) = x$, $T_{k+1}(x) = 2xT_k(x) - T_{k-1}(x)$, define damped moments on \tilde{A} :

$$s_k(A) = \text{tr}(T_k(\tilde{A})), \quad \hat{s}_k(A) = e^{-\eta k} s_k(A). \quad (2)$$

Hutchinson with p probes z_i ($\mathbb{E}[z_i z_i^\top] = I$) estimates traces:

$$\hat{\text{tr}}(M) = \frac{1}{p} \sum_{i=1}^p z_i^\top M z_i, \quad y_0 = z_i, \quad y_1 = \tilde{A} z_i,$$

$$y_{k+1} = 2\tilde{A} y_k - y_{k-1},$$

so the cost is $O(pK \text{cost}(\tilde{A}\mathbf{v}))$.

Compact spectral fingerprints (CSF/ASF-H). For target K , form $d \in \mathbb{R}^K$ with

$$d_0 := w_0 \quad (\text{default } w_0 = n \text{ in our experiments;}$$

$$\text{a size-neutral variant uses } w_0 = 1),$$

and define the ℓ_2 -normalized fingerprint

$$\phi_K(A) = \frac{(d_0, \dots, d_{K-1})}{\|(d_0, \dots, d_{K-1})\|_2} \in \mathbb{R}^K. \quad (3)$$

Exact traces give *CSF*; Hutchinson gives *CSF-H*. The adaptive variant (*ASF*) chooses K via a Hankel-ratio and an energy gate (Section 3).

Distances and evaluation. Unless noted, we use **Euclidean** distance between ℓ_2 -normalized fingerprints (cosine reported as an ablation; *E6/E6+ uses cosine*). Clustering quality is measured by ARI and mean silhouette from the pairwise distance matrix.

3 Methodology: Compact/Adaptive Spectral Fingerprints

Goal. Given a (typically symmetric or symmetrizable) matrix $A \in \mathbb{R}^{n \times n}$, we seek a compact fingerprint $\phi(A) \in \mathbb{R}^{K^*}$ that (i) is invariant to similarity/permutation/diagonal similarity transforms; (ii) is robust to noise and positive scaling; (iii) is computable in $\mathcal{O}(pK \text{nnz}(A))$ using only sparse matvecs; and (iv) adapts K_* via data-driven stopping.

3.1 Preliminaries and Notation

Let T_k be Chebyshev polynomials of the first kind ($T_0(x) = 1$, $T_1(x) = x$, $T_{k+1}(x) = 2xT_k(x) - T_{k-1}(x)$). We write $\text{tr}(\cdot)$ for the trace, $\|\cdot\|_2$ for the spectral norm, and $\|\cdot\|_F$ for the Frobenius norm.

Affine normalization to $[-1, 1]$. We use the affine map in Eq. (1) with a small relative margin ε_{rel} ; for markedly non-Hermitian inputs we use radius scaling or symmetrization (see Section 2).

Implementation note. To obtain similarity-invariant scaling, we estimate only scalar spectral endpoints or a 2-norm bound—no eigenvectors or full spectra. On small dense inputs we may call an eigenvalue routine solely for endpoints (no eigenvectors); on large runs we use matvec-only bounds (power/Lanczos or Gershgorin). CSF/ASF themselves use matvec-based Chebyshev recurrences.

3.2 Fixed- K Chebyshev Spectral Fingerprints (CSF)

For fixed $K \geq 1$ and damping $\eta > 0$, define

$$\phi_K(A) = [d_0, \dots, d_{K-1}], \quad d_k = e^{-\eta k} \text{tr}(T_k(\tilde{A})).$$

To avoid size leakage across different n , set

$$d_0 \triangleq w_0, \quad \text{default } w_0 = 1 \quad (\text{size-neutral});$$

the classical choice $w_0 = n$ and very small $w_0 \ll 1$ are also supported. *We used $w_0 = n$ in our experiments unless otherwise stated (see Section 1).* Finally, L2-normalize $\phi_K(A) \leftarrow \phi_K(A) / \|\phi_K(A)\|_2$.

Algorithm 1 CSF-K (Fixed- K Chebyshev Fingerprint; matrix form. At scale we use Hutchinson *matvec* recurrences.)

Require: A , target $K \geq 1$, damping $\eta > 0$, w_0 (default = 1)

- 1: $\tilde{A} \leftarrow \text{SCALETOUNITINTERVAL}(A)$
- 2: $T_{\text{prev}} \leftarrow I, T_{\text{curr}} \leftarrow \tilde{A}$
- 3: $d_0 \leftarrow w_0$
- 4: **if** $K > 1$ **then**
- 5: $d_1 \leftarrow e^{-\eta} \text{tr}(\tilde{A})$
- 6: **end if**
- 7: **for** $k = 2$ to $K - 1$ **do**
- 8: $T_{\text{next}} \leftarrow 2\tilde{A}T_{\text{curr}} - T_{\text{prev}}$
- 9: $d_k \leftarrow e^{-\eta k} \text{tr}(T_{\text{next}})$
- 10: $T_{\text{prev}} \leftarrow T_{\text{curr}}, T_{\text{curr}} \leftarrow T_{\text{next}}$
- 11: **end for**
- 12: **return** $\phi_K(A)$ \leftarrow

$$[d_0, \dots, d_{K-1}] / \|[d_0, \dots, d_{K-1}]\|_2$$

3.3 Adaptive Spectral Fingerprints (ASF)

ASF produces $\phi_{K_*}(A)$ by a *dual stopping rule*: (i) an **energy-tail** criterion; and (ii) a **Hankel low-rank** detector.

Energy-tail rule. Let $E_k = \sum_{j=0}^k d_j^2$ and $\rho_k = d_k^2 / (E_k + \varepsilon)$ with a tiny stabilizer $\varepsilon > 0$. If $\rho_k < \tau$ for w consecutive $k \geq K_{\min}$, stop at $K_* = k + 1$.

Hankel low-rank rule (with stabilization). Form a Hankel H from $\{d_0, \dots, d_k\}$ with $H_{ij} = d_{i+j}$, $n_H = \lfloor (k+1)/2 \rfloor$. For numerical stability we (i) L2-normalize (d_j) before forming H , (ii) optionally use a *scaled Hankel* (row/column normalization), and (iii) estimate the ratio $r_H = \sigma_{\min}(H_\lambda) / \sigma_{\max}(H_\lambda)$ via Tikhonov-regularized $H_\lambda = \begin{bmatrix} H \\ \sqrt{\lambda}I \end{bmatrix}$ (e.g., $\lambda \approx 10^{-10}$) or incremental/randomized SVD. If $r_H < \varepsilon_H$ for w steps and $k \geq K_{\min}$, stop.

Decision logic. Take the earliest $k \geq K_{\min}$ that satisfies either rule for w consecutive steps.

Algorithm 2 ASF (Adaptive, exact traces)

Require: $A, K_{\min}, K_{\max}, \eta$, thresholds (τ, ε_H) , window w, w_0 (default = 1)

- 1: $\tilde{A} \leftarrow \text{SCALETOUNITINTERVAL}(A)$ \triangleright for symmetric A ; non-Hermitian uses unit-disk scaling
- 2: $T_{\text{prev}} \leftarrow I, T_{\text{curr}} \leftarrow \tilde{A}$
- 3: $d_0 \leftarrow w_0; E_0 \leftarrow d_0^2; h \leftarrow 0$
- 4: **if** $K_{\min} > 1$ **then**
- 5: $d_1 \leftarrow e^{-\eta} \text{tr}(\tilde{A}); E_1 \leftarrow E_0 + d_1^2$
- 6: **end if**
- 7: **for** $k = 2$ to $K_{\max} - 1$ **do**
- 8: $T_{\text{next}} \leftarrow 2\tilde{A}T_{\text{curr}} - T_{\text{prev}}$
- 9: $d_k \leftarrow e^{-\eta k} \text{tr}(T_{\text{next}}); E_k \leftarrow E_{k-1} + d_k^2$
- 10: $\rho_k \leftarrow d_k^2 / (E_k + \varepsilon)$
- 11: Build stabilized H from $\{d_0, \dots, d_k\}$; $r_H \leftarrow \sigma_{\min}(H_\lambda) / \sigma_{\max}(H_\lambda)$
- 12: $\text{HIT} \leftarrow (\rho_k < \tau \vee r_H < \varepsilon_H) \wedge (k + 1 \geq K_{\min})$
- 13: $h \leftarrow \text{HIT}?(h + 1) : 0$
- 14: **if** $h \geq w$ **then**
- 15: $K_* \leftarrow k + 1$; **break**
- 16: **end if**
- 17: $T_{\text{prev}} \leftarrow T_{\text{curr}}, T_{\text{curr}} \leftarrow T_{\text{next}}$
- 18: **end for**
- 19: **return** $\phi_{K_*}(A)$ \leftarrow

$$[d_0, \dots, d_{K_*-1}] / \|[d_0, \dots, d_{K_*-1}]\|_2$$

3.4 Hutchinson–Chebyshev for Large Sparse Matrices

For large A , traces are estimated with Hutchinson probes: draw $z^{(i)} \in \{\pm 1\}^n$ (or $z^{(i)} \sim \mathcal{N}(0, I)$) and set

$$\widehat{\text{tr}}(T_k(\tilde{A})) = \frac{1}{p} \sum_{i=1}^p (z^{(i)})^\top u_k^{(i)}, \quad u_0^{(i)} = z^{(i)},$$

$$u_1^{(i)} = \tilde{A}z^{(i)}, \quad u_{k+1}^{(i)} = 2\tilde{A}u_k^{(i)} - u_{k-1}^{(i)}.$$

Define $\widehat{d}_k = e^{-\eta k} \widehat{\text{tr}} T_k(\cdot)$ and the SE-guarded energy ratio

$$\widehat{\rho}_k = \frac{\widehat{d}_k^2}{\sum_{j \leq k} \widehat{d}_j^2 + \varepsilon} \quad \text{and stop if } \widehat{\rho}_k < \tau(1 + \gamma \cdot \text{relSE}_k),$$

where $\text{relSE}_k = \text{se}_k / (|\widehat{d}_k| + \varepsilon)$, $\gamma \in [2, 3]$. We use a small window w and a fixed γ as a simple sequential guard; more formal error-rate control (e.g., α -spending) is left to future work.

Algorithm 3 ASF-H (Adaptive, Hutchinson)

Require: A , p probes, K_{\min} , K_{\max} , η , (τ, ε_H) , w , SE-guard γ , w_0 (default = 1)

- 1: $\widetilde{A} \leftarrow \text{SCALETOUNITINTERVAL}(A)$
- 2: For each probe i : $u_0^{(i)} \leftarrow z^{(i)}$, $u_1^{(i)} \leftarrow \widetilde{A}z^{(i)}$
- 3: $\widehat{d}_0 \leftarrow w_0$, $\widehat{E}_0 \leftarrow \widehat{d}_0^2$, $h \leftarrow 0$
- 4: **if** $K_{\min} > 1$ **then**
- 5: $\widehat{t}_1 \leftarrow \frac{1}{p} \sum_i \langle z^{(i)}, u_1^{(i)} \rangle$, $\widehat{d}_1 \leftarrow e^{-\eta} \widehat{t}_1$, $\widehat{E}_1 \leftarrow \widehat{E}_0 + \widehat{d}_1^2$
- 6: **end if**
- 7: **for** $k = 2$ to $K_{\max} - 1$ **do**
- 8: **for** each i **do**
- 9: $u_{k+1}^{(i)} \leftarrow 2\widetilde{A}u_k^{(i)} - u_{k-1}^{(i)}$
- 10: **end for**
- 11: $\widehat{t}_k \leftarrow \frac{1}{p} \sum_i \langle z^{(i)}, u_k^{(i)} \rangle$, $\widehat{d}_k \leftarrow e^{-\eta k} \widehat{t}_k$, $\widehat{E}_k \leftarrow \widehat{E}_{k-1} + \widehat{d}_k^2$
- 12: Estimate se_k ; set $\text{relSE}_k \leftarrow \text{se}_k / (|\widehat{d}_k| + \varepsilon)$
- 13: Build stabilized H from $\{\widehat{d}_0, \dots, \widehat{d}_k\}$; $r_H \leftarrow \sigma_{\min}(H_\lambda) / \sigma_{\max}(H_\lambda)$
- 14: $\text{HIT} \leftarrow \left(\widehat{d}_k^2 / \widehat{E}_k < \tau(1 + \gamma \cdot \text{relSE}_k) \vee r_H < \varepsilon_H \right) \wedge (k + 1 \geq K_{\min})$
- 15: $h \leftarrow \text{HIT}?(h + 1) : 0$
- 16: **if** $h \geq w$ **then**
- 17: $K_* \leftarrow k + 1$; **break**
- 18: **end if**
- 19: **end for**
- 20: **return** $\phi_{K_*}(A) \leftarrow [\widehat{d}_0, \dots, \widehat{d}_{K_*-1}] / \|\widehat{d}_0, \dots, \widehat{d}_{K_*-1}\|_2$

Remark 1 (Scope of the claim). Our claims concern avoiding *eigenvectors* or *full eigen-spectra*. Scalar endpoint/radius estimates (via power/Lanczos, Gershgorin, or small-matrix eigenvalue calls) do not contradict this scope and are not required by the method.

3.5 Similarity Metrics and Multi-view Postprocessing

By default we use Euclidean distance between ℓ_2 -normalized fingerprints; cosine is reported as an ablation. In the E6/E6+ recommender experiments we

used *cosine* distance (Euclidean is included as an ablation). When class covariances are heterogeneous, a whitened (Mahalanobis) metric can improve separation. For nonsymmetric inputs, use $H = \frac{1}{2}(A + A^\top)$ or $A^\top A$; multiple views (e.g., adjacency and normalized Laplacian) can be concatenated or fused by late averaging (see Appendix for details).

3.6 Complexity and Memory

Let c_{mv} be the cost of one sparse matvec with A . CSF (exact trace): $\mathcal{O}(K c_{\text{mv}})$ if traces are available; at scale we use Hutchinson. ASF-H: $\mathcal{O}(pK c_{\text{mv}})$ time and, with streaming/batching, $\mathcal{O}(n)$ memory (otherwise $\mathcal{O}(pn)$ if all probe states are kept simultaneously). Small Hankel updates are $\mathcal{O}(K^2)$ and negligible for $K \leq 64$.

4 Theory: Properties and Guarantees

Setup. Let A be real symmetric (or symmetrized as in Sec. 2) and define \widetilde{A} by Eq. (1) so that $\text{spec}(\widetilde{A}) \subset [-1, 1]$. Let T_k be Chebyshev polynomials, $s_k = e^{-\eta k} \text{tr}(T_k(\widetilde{A}))$, $E_k = \sum_{j=0}^k s_j^2$, $e_k = s_k^2 / (E_k + \varepsilon)$, and let H_k be the Hankel from (s_0, \dots, s_k) with ratio $r_k = \sigma_{\min}(H_k) / \sigma_{\max}(H_k)$. The fingerprint is $\phi_K(A) = [s_0, \dots, s_{K-1}] / \|[s_0, \dots, s_{K-1}]\|_2$.

Proposition 2 (Invariance). *For any invertible S , permutation P , positive diagonal D , and $\alpha > 0$, moments (hence ϕ_K) are invariant:*

$$s_k(S^{-1}AS) = s_k(A), \quad s_k(P^\top AP) = s_k(A),$$

$$s_k(D^{-1}AD) = s_k(A), \quad s_k(\alpha A) = s_k(A).$$

Proof: App. B.

Theorem 3 (Adaptive compactness: stopping & tail control). *Fix $\tau_e \in (0, 1)$, $\tau_h > 0$, window w , $K_{\min} \geq 1$. If either (i) $e_k < \tau_e$ or (ii) $r_k < \tau_h$ holds for w consecutive $k \geq K_{\min}$, Algorithm 2 returns $K^* \leq k^* + w$ for some such k^* ; moreover, under (i) the normalized tail energy obeys*

$$\frac{\sum_{j>t} s_j^2}{E_t + \sum_{j>t} s_j^2} \leq \frac{\tau_e}{1 - \tau_e}.$$

Proof: App. B (uses Prop. 10).

Proposition 4 (Hankel low rank: mixture-of-modes). *Suppose (s_k) arises from a mixture of r damped exponential/cosine modes with noise variance σ^2 : $s_k = \sum_{i=1}^r a_i \rho_i^k \cos(k\theta_i + \varphi_i) + \xi_k$, with $|\rho_i| \leq 1$ and $\mathbb{E}\xi_k = 0$, $\text{Var}(\xi_k) = \sigma^2$. Then in the noiseless case ($\sigma = 0$) one has $\text{rank}(H_L) \leq r$ for all L (under the convention that one cosine mode counts a complex-conjugate pair as a single mode). With noise, for any fixed L we have $r_L = \sigma_{\min}(H_L) / \sigma_{\max}(H_L) \rightarrow 0$ as $\sigma \rightarrow 0$.*

Consequently, for any $\tau_h > 0$ there exists $\sigma_0 = \sigma_0(\tau_h, L, r, \{a_i, \rho_i, \theta_i, \varphi_i\}) > 0$ such that if $\sigma < \sigma_0$ then $r_L < \tau_h$. Proof: App. B.

Remark 5 (Counting convention). A single real cosine mode $a \rho^k \cos(k\theta + \varphi)$ equals the real part of two complex exponentials with conjugate nodes. If one counts complex-conjugate pairs separately, the Hankel rank bound becomes $\text{rank}(H_L) \leq 2r$; our statement uses the common convention that a conjugate pair is counted as one “mode”, hence the bound $\leq r$.

Theorem 6 (Hutchinson concentration). *Let $B_k = T_k(\tilde{A})$ and $\hat{t}_k = \frac{1}{p} \sum_{i=1}^p (z^{(i)})^\top B_k z^{(i)}$ with i.i.d. Rademacher probes. For any $\delta \in (0, 1)$,*

$$|\hat{t}_k - \text{tr}(B_k)| \leq \|B_k\|_F \sqrt{\frac{2 \log(2/\delta)}{p}},$$

$$|\hat{s}_k - s_k| \leq e^{-\eta k} \|B_k\|_F \sqrt{\frac{2 \log(2/\delta)}{p}}.$$

(Uniform-in- k version up to K in App., Cor. 11.) Proof: App. B.

Theorem 7 (Lipschitz stability). *If $\text{spec}(\tilde{A}), \text{spec}(\tilde{B}) \subset [-1, 1]$, then for all $k \geq 0$,*

$$|\text{tr} T_k(\tilde{A}) - \text{tr} T_k(\tilde{B})| \leq n C_T k^2 \|\tilde{A} - \tilde{B}\|_2 \quad (C_T \leq 2),$$

and for any $K \geq 1$,

$$\begin{aligned} \|\phi_K(A) - \phi_K(B)\|_2 &\leq \\ \frac{n}{\|[s_0, \dots, s_{K-1}]\|_2} &\left(\sum_{k=0}^{K-1} e^{-2\eta k} C_T^2 k^4 \right)^{1/2} \|\tilde{A} - \tilde{B}\|_2 \\ &= \mathcal{O}(n \eta^{-5/2} \|\tilde{A} - \tilde{B}\|_2). \end{aligned}$$

Proof: App. B.

5 Experiments

We evaluate on synthetic suites (E0–E2), strong baselines (E2b), a SuiteSparse mini-benchmark (E3), Hutchinson ablations (E4), noise stability (E5), and an adversarial preconditioner-selection stress test (E6/E6+). Unless noted, we use Euclidean distance on ℓ_2 -normalized fingerprints (cosine is an ablation), CSF with $w_0=1$ and small damping $\eta > 0$.

5.1 E0: Invariance & Scaling (tables only)

We test permutation, (diagonal/general) similarity, and positive scaling with/without our spectral normalization. With normalization (*scaled*), all transforms collapse to ≈ 0 distance (below the numerical floor); without normalization, only positive scaling (**alpha**) breaks invariance.

Table 1: E0 (scaled): distance to original after transform (mean/median/IQR). All are ≈ 0 (below numerical floor, $< 10^{-15}$).

transform	mean	median	IQR
alpha	0.0	0.0	0.0
diag_sim	0.0	0.0	0.0
gen_sim	0.0	0.0	0.0
perm	0.0	0.0	0.0

Table 2: E0 (no-scale): positive scaling breaks invariance; others remain zero.

transform	mean	median	IQR
alpha	0.9782	1.3316	1.3015
diag_sim	0.0000	0.0000	0.0000
gen_sim	0.0000	0.0000	0.0000
perm	0.0000	0.0000	0.0000

5.2 E1: 4-Family Compactness (tables only)

We sweep K and compare CSF/ASF to spectral/entrywise baselines. CSF- $K=3, 5$ achieve **ARI** = 1.0 with top silhouettes and lowest runtimes; ASF (exact) also reaches **ARI** = 1.0; Hutchinson (ASF-H) preserves accuracy at higher cost.

Table 3: E1 K-sweep: ARI / silhouette / runtime (s).

method	K or m	ARI	Silhouette	runtime
ASF (Adaptive, exact trace)	–	1.0000	0.8510	0.0692
ASF-H (Adaptive, Hutchinson)	–	1.0000	0.8555	4.2217
CSF-K (Fixed-K Chebyshev)	3	1.0000	0.8928	0.0431
CSF-K (Fixed-K Chebyshev)	5	1.0000	0.8942	0.0457
CSF-K (Fixed-K Chebyshev)	10	1.0000	0.8550	0.0632
CSF-K (Fixed-K Chebyshev)	50	1.0000	0.8100	0.2068
Baseline: Raw Power Moments	10	1.0000	0.8755	0.0562
Baseline: Spectral Norm $\ \cdot\ _2$	–	0.6508	0.7505	–
Baseline: Top- m Eigenvalues	16	0.6220	0.6814	0.0635
Baseline: Heat-Trace @ T	–	0.5041	0.5492	0.0584
Baseline: Frobenius	–	0.3260	0.3028	–
CSF-K (Fixed-K Chebyshev)	1	0.0020	0.0000	0.0598

Table 4: E1: Adaptive K^* summary (ASF).

	mean	median	IQR
K^*	8.39	9.0	3.0

5.3 E2: 5-Family (BA vs. ER included)

On a harder 5-family suite, CSF- $K=5$ and ASF both reach **ARI** = 1.0. We report overall and per-view silhouettes.

Table 5: E2: Per-method scores.

method	ARI	Silh. (overall)	Silh. [Cov]	Silh. [Kernel]	Silh. [GOE]	Silh. [Adj-BA]	Silh. [Adj-ER]
ASF (Adaptive, exact)	1.0000	0.7989	0.8160	0.8207	0.8591	0.7248	0.7737
CSF-K (Fixed-K)	1.0000	0.8209	0.9054	0.8642	0.8466	0.7699	0.7184
Baseline: Top- m Eigen	0.6933	0.5855	0.8850	0.8126	0.6057	0.2727	0.3513
Baseline: Heat-Trace	0.4583	0.6048	0.8502	0.7710	0.4504	0.4569	0.4957

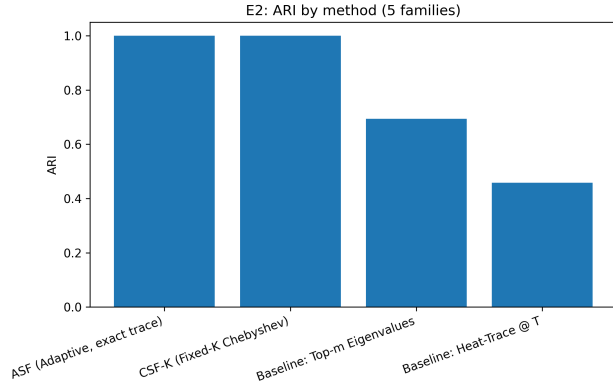


Figure 1: E2: ARI/silhouette overview across methods and views.

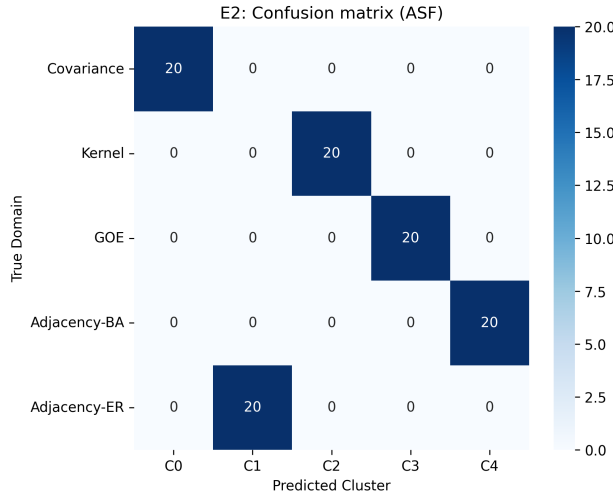


Figure 2: E2: Confusion matrix (one run; label permutations allowed). $ARI = 1.0$.

5.4 E2b: Strong Baselines

CSF- $K=5$ matches the best accuracy ($ARI = 1.0$) while using only 5 dimensions and avoiding eigendecomposition.

Table 6: E2b: Accuracy vs. feature dimension vs. time; eigendecomposition required?

method	ARI	Silh.	Dim	runtime (s)	Eigendecomp
CSF- $K=5$ (ours)	1.000	0.8209	5	0.0604	No
ASF (ours)	1.000	0.7989	8	0.0875	No
EigenHist+Wasserstein	1.000	0.7738	64	0.3573	Yes
WL-Subtree (graphs)	1.000	0.3067	9153	0.0582	No
HeatKernel (L2 on traces)	0.773	0.7005	5	0.0758	Yes

5.5 E3: SuiteSparse Mini-Benchmark (Hutchinson)

On four real matrices, both CSF-H and ASF-H achieve $ARI = 1.0$, validating sketch-based fingerprints. Specifically, we use HB/bcsstk01, HB/bcsstk06, HB/gr_30_30, and AG-Monien/netz4504 from the SuiteSparse Matrix Collection.

Table 7: E3: SuiteSparse mini-benchmark.

method	ARI	Silhouette
CSF-K (Hutchinson)	1.0	0.6220
ASF-H (Adaptive, Hutchinson)	1.0	0.5386

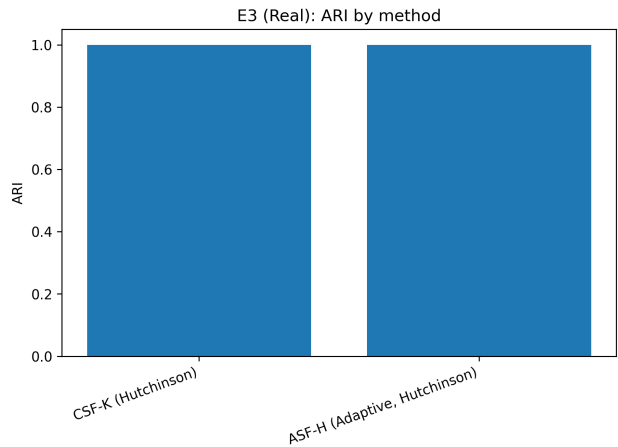


Figure 3: E3: ARI on SuiteSparse (Hutchinson).

5.6 E4: Hutchinson Ablation (probe count p)

ARI remains at **1.0** across all p and $K \in \{3, 5\}$; silhouette increases smoothly; runtime scales near-linearly.

Table 8: E4: ARI vs. p (columns are K).

p	$K=3$	$K=5$
10	1.0	1.0
50	1.0	1.0
100	1.0	1.0
200	1.0	1.0
500	1.0	1.0
1000	1.0	1.0

Table 9: E4: Silhouette vs. p (columns are K).

p	$K=3$	$K=5$
10	0.8740	0.8587
50	0.8894	0.8801
100	0.8899	0.8899
200	0.8910	0.8904
500	0.8914	0.8946
1000	0.8935	0.8941

Table 10: E4: Runtime (s) vs. p (columns are K).

p	$K=3$	$K=5$
10	0.0787	0.0893
50	0.1896	0.2410
100	0.3223	0.4385
200	0.5984	0.8278
500	1.3878	1.9215
1000	2.7560	2.7219

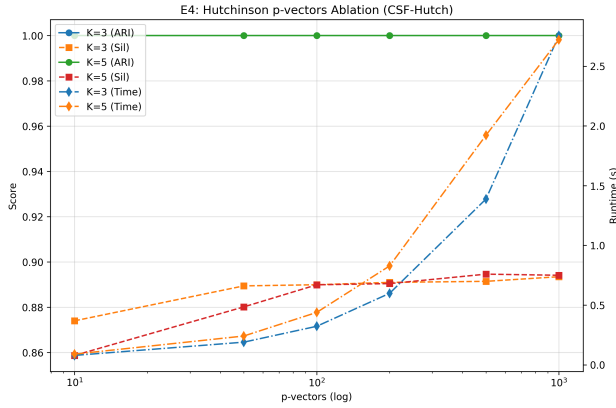


Figure 4: E4: Probe-quality-time trade-off for CSF-H/ASF-H.

5.7 E5: Noise Stability

Fingerprint distance scales $\propto \epsilon^{1.03}$ with additive noise; fit $R^2 \approx 0.993$.

Table 11: E5: Noise-distance regression (log-log).

Metric	Value
Slope	1.0289
R^2	0.9931

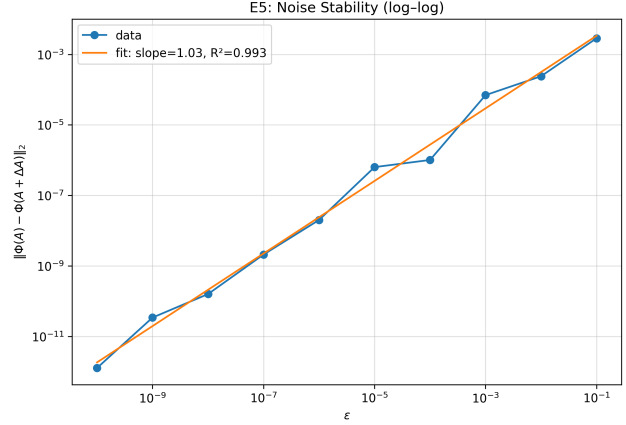


Figure 5: E5: Log-log fit of fingerprint distance vs. noise level ϵ .

5.8 E6/E6+: Trap-Robust Preconditioner Selection

Across adversarial seeds, the phylogeny-guided policy attains **success rate 1.00** with **p90 regret = 0**; Frobenius 1-NN exhibits **p90 = 34** extra iterations.

Table 12: E6+: Aggregated adversarial results (success and regret).

Metric	Value
Phy Success Rate	1.00
Fro-1NN Success Rate	0.75
Fro- k NN Success Rate	0.95
Phy Extra Iters (Median)	0.00
Fro-1NN Extra Iters (Median)	0.00
Fro- k NN Extra Iters (Median)	0.00
Phy Extra Iters (Mean)	0.00
Fro-1NN Extra Iters (Mean)	5.70
Fro- k NN Extra Iters (Mean)	4.55
Phy Extra Iters (p90)	0.00
Fro-1NN Extra Iters (p90)	34.00
Fro- k NN Extra Iters (p90)	0.00

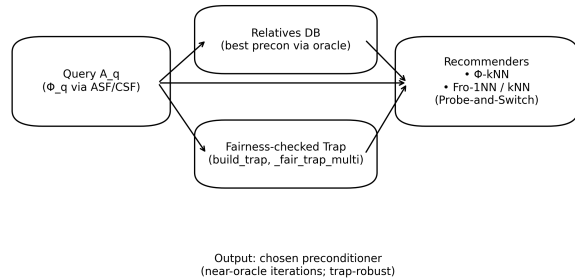


Figure 6: E6: Probe-and-Switch flow (trap detection and switching).

6 Related Work

Spectral fingerprints and graph descriptors.

Permutation-invariant spectral summaries are long-standing. Heat-trace descriptors capture multiscale diffusion (e.g., NetLSD) and compare graphs without node alignment (Tsitsulin et al., 2018). Eigenvalue histograms compared by optimal transport (e.g., Wasserstein) are effective but typically require (partial) eigendecompositions and careful binning (Villani, 2008). Weisfeiler–Lehman subtree kernels (Shervashidze et al., 2011) encode rich combinatorics yet are not similarity-invariant and can be fragile outside the WL regime. Our CSF/ASF fingerprints avoid computing eigenvectors or full eigen-spectra, operate via matvecs, and are invariant to permutation, similarity, and positive scaling.

Chebyshev expansions and stochastic traces.

Chebyshev/KPM expansions approximate spectral densities and traces from matrix–vector products (Weiße et al., 2006). Hutchinson’s estimator and refinements (Hutch++) enable scalable trace estimation with variance $\mathcal{O}(1/p)$ for p probe vectors (Hutchinson, 1989; Meyer et al., 2021). Stochastic Lanczos quadrature provides complementary density-of-states estimates (Ubaru et al., 2017). These techniques sit within randomized numerical linear algebra (Halko et al., 2011). We combine affine spectrum mapping, damped Chebyshev moments, and Hutchinson sketches into compact, similarity-invariant fingerprints.

Preconditioning and automated choices. Classical work shows the centrality of preconditioning for Krylov solvers (CG, GMRES) (Hestenes and Stiefel, 1952; Meijerink and van der Vorst, 1977; Trottenberg et al., 2001; Saad, 2003; Benzi, 2002). Prior auto-tuning often relies on heavy spectral surrogates or metadata. Our *matrix phylogeny* is orthogonal: a retrieval layer built from compact fingerprints that steers a probe-and-switch policy, achieving near-oracle iteration counts without eigenspectra.

Limits of spectral identifiability. Cospectral non-isomorphic graphs (and matrices) exist (van Dam and Haemers, 2003); descriptors depending only on spectra, including ours, cannot distinguish them in principle. We mitigate empirically via multi-view fingerprints (adjacency/Laplacian/GOE/kernel) and find strong separation across families.

7 Limitations

Cospectral ambiguity. Spectral equivalence remains a worst-case confound; multi-view concatenation helps

but cannot resolve all cases.

Endpoint/scaling estimates. Chebyshev stability hinges on mapping spectra to $[-1, 1]$. Overly loose bounds can overdamp higher moments, sometimes requiring a slightly larger K or ASF’s adaptive stop.

Sketch variance. Hutchinson estimates concentrate as $1/\sqrt{p}$; high-variance instances may need more probe vectors to stabilize ASF’s stopping rule.

Nonsymmetric inputs. For non-Hermitian A we use radius scaling or symmetrization $(A^\top A$ or $(A+A^\top)/2$). This preserves invariances but may blur non-normal features when they matter.

Actionability scope. Our auto-selection uses a standard preconditioner portfolio; specialized domains may benefit from broader candidates or lightweight non-spectral cues (e.g., sparsity sketches).

8 Conclusion

We presented *Matrix Phylogeny* via **Compact/Adaptive Spectral Fingerprints** (CSF/ASF): tiny ($K \leq 10$), eigendecomposition-free, and invariant descriptors built from Chebyshev moments and Hutchinson sketches. Across E0–E6+, we observe *phylogenetic compactness*: **CSF- $K=3-5$** already yields perfect clustering on synthetic and real suites while being fastest, and **ASF** provides a conservative safety net (median $K^* \approx 9$). The fingerprints are stable to perturbations (noise–distance slope ≈ 1.03 , $R^2 \approx 0.993$) and power an actionable pipeline: a nearest-neighbor *probe-and-switch* recommender attains near-oracle iterations in adversarial settings, avoiding the trap behavior seen with Frobenius baselines.

The recipe—affine scaling to $[-1, 1]$, Chebyshev recurrences, Hutchinson sketches, cosine distances—unlocks scalability, invariance, and accuracy with feature dimensions far smaller than spectral baselines. We recommend **CSF- $K=5$** as the default and **ASF** when domain adaptivity is required. Future work: principled multi-view fusion, solver-in-the-loop tuning of damping/stopping/distances for regret, and identifiability theory for when compact moments uniquely determine matrix families.

References

- Benzi, M. (2002). Preconditioning techniques for large linear systems: A survey. *Journal of Computational Physics*, 182(2).
- Halko, N., Martinsson, P.-G., and Tropp, J. A. (2011). Finding structure with randomness: Probabilistic algorithms for constructing approximate matrix decompositions. *SIAM Review*, 53(2).
- Hestenes, M. R. and Stiefel, E. (1952). Methods of conjugate gradients for solving linear systems. *Journal of Research of the National Bureau of Standards*, 49(6).
- Hutchinson, M. F. (1989). A stochastic estimator of the trace of the influence matrix for laplacian smoothing splines. *Communications in Statistics – Simulation and Computation*, 18(3).
- Meijerink, J. A. and van der Vorst, H. A. (1977). An iterative solution method for linear systems of which the coefficient matrix is a symmetric m-matrix. *Mathematics of Computation*, 31.
- Meyer, A., Musco, C., Musco, C., and Woodruff, D. P. (2021). Hutch++: Optimal stochastic trace estimation. In *Proceedings of the 2021 ACM-SIAM Symposium on Discrete Algorithms (SODA)*.
- Saad, Y. (2003). *Iterative Methods for Sparse Linear Systems*. SIAM, Philadelphia, 2 edition.
- Shervashidze, N., Schweitzer, P., van Leeuwen, E. J., Mehlhorn, K., and Borgwardt, K. M. (2011). Weisfeiler–Lehman graph kernels. *Journal of Machine Learning Research*, 12.
- Trottenberg, U., Oosterlee, C. W., and Schüller, A. (2001). *Multigrid*. Academic Press, San Diego.
- Tsitsulin, A., Mottin, D., Karras, P., Bronstein, A., and Müller, E. (2018). NetLSD: Hearing the shape of a graph. In *Proceedings of the 24th ACM SIGKDD International Conference on Knowledge Discovery and Data Mining*.
- Ubaru, S., Chen, J., and Saad, Y. (2017). Fast estimation of $\text{tr}(f(A))$ via stochastic lanczos quadrature. *SIAM Journal on Matrix Analysis and Applications*, 38(4).
- van Dam, E. R. and Haemers, W. H. (2003). Which graphs are determined by their spectrum? *Linear Algebra and its Applications*, 373.
- Villani, C. (2008). *Optimal Transport: Old and New*, volume 338 of *Grundlehren der mathematischen Wissenschaften*. Springer, Berlin, Heidelberg.
- Weiß, A., Wellein, G., Alvermann, A., and Fehske, H. (2006). The kernel polynomial method. *Reviews of Modern Physics*, 78(1).

Reproducibility Checklist

1. For all models and algorithms presented, check if you include:
 - (a) A clear description of the mathematical setting, assumptions, algorithm, and/or model. [Yes]
 - (b) An analysis of the properties and complexity (time, space, sample size) of any algorithm. [Yes]
 - (c) (Optional) Anonymized source code, with specification of all dependencies, including external libraries. [Yes]
2. For any theoretical claim, check if you include:
 - (a) Statements of the full set of assumptions of all theoretical results. [Yes]
 - (b) Complete proofs of all theoretical results. [Yes]
 - (c) Clear explanations of any assumptions. [Yes]
3. For all figures and tables that present empirical results, check if you include:
 - (a) The code, data, and instructions needed to reproduce the main experimental results (either in the supplemental material or as a URL). [Yes]
 - (b) All the training details (e.g., data splits, hyperparameters, how they were chosen). [Yes]
 - (c) A clear definition of the specific measure or statistics and error bars (e.g., with respect to the random seed after running experiments multiple times). [Yes]
 - (d) A description of the computing infrastructure used. (e.g., type of GPUs, internal cluster, or cloud provider). [Yes]
4. If you are using existing assets (e.g., code, data, models) or curating/releasing new assets, check if you include:
 - (a) Citations of the creator If your work uses existing assets. [Yes]
 - (b) The license information of the assets, if applicable. [Not Applicable]
 - (c) New assets either in the supplemental material or as a URL, if applicable. [Not Applicable]
 - (d) Information about consent from data providers/curators. [Not Applicable]
 - (e) Discussion of sensible content if applicable, e.g., personally identifiable information or offensive content. [Not Applicable]

5. If you used crowdsourcing or conducted research with human subjects, check if you include:
 - (a) The full text of instructions given to participants and screenshots. [Not Applicable]
 - (b) Descriptions of potential participant risks, with links to Institutional Review Board (IRB) approvals if applicable. [Not Applicable]
 - (c) The estimated hourly wage paid to participants and the total amount spent on participant compensation. [Not Applicable]

A Appendix: Theoretical Guarantees and Implementation Details

A.1 Notation and Theorem Environments

We assume throughout that $A \in \mathbb{R}^{n \times n}$ is real symmetric (or is symmetrized as $H = \frac{1}{2}(A + A^\top)$ or $A^\top A$). Let the affine spectral normalization be

$$\begin{aligned}\tilde{A} &= \frac{A - mI}{r}, & m &= \frac{1}{2}(\lambda_{\max}(A) + \lambda_{\min}(A)), \\ r_0 &= \frac{1}{2}(\lambda_{\max}(A) - \lambda_{\min}(A)), & r &= (1 + \varepsilon_{\text{rel}})r_0,\end{aligned}$$

with a tiny relative margin $\varepsilon_{\text{rel}} > 0$, so that $\text{spec}(\tilde{A}) \subset [-1, 1]$ and scaling $A \mapsto \alpha A$ leaves \tilde{A} unchanged. We write T_k for the Chebyshev polynomials of the first kind, $T_0(x) = 1$, $T_1(x) = x$, $T_{k+1}(x) = 2xT_k(x) - T_{k-1}(x)$. Define the (optionally damped) moments $s_k(A) = e^{-\eta k} \text{tr}(T_k(\tilde{A}))$, cumulative energy $E_K(A) = \sum_{k=0}^K s_k(A)^2$, energy share $e_k = s_k^2/(E_k + \varepsilon)$, and Hankel ratio $r_k = \sigma_{\min}(H_k)/\sigma_{\max}(H_k)$ for $H_k = [s_{i+j}]_{i,j=0}^{\lfloor k/2 \rfloor}$. The fingerprint is $\phi_K(A) = [s_0, \dots, s_{K-1}]/\|[s_0, \dots, s_{K-1}]\|_2$, and K^* is selected by Algorithm 2.

Proposition 8 (Invariance (appendix)). *Let S be invertible, P a permutation (orthogonal), D positive diagonal, and $\alpha > 0$. With the relative-margin normalization above, for all $k \geq 0$,*

$$\begin{aligned}\text{tr } T_k((S^{-1}AS)^\sim) &= \text{tr } T_k(\tilde{A}), \\ \text{tr } T_k((P^\top AP)^\sim) &= \text{tr } T_k(\tilde{A}), \\ \text{tr } T_k((D^{-1}AD)^\sim) &= \text{tr } T_k(\tilde{A}),\end{aligned}$$

and $\text{tr } T_k((\alpha A)^\sim) = \text{tr } T_k(\tilde{A})$. Consequently $\phi_K(\cdot)$ computed on \tilde{A} is invariant to similarity, permutations, diagonal similarities, and global positive scaling.

Proof sketch. Polynomials conjugate: $T_k(S^{-1}AS) = S^{-1}T_k(A)S$ and tr is conjugation-invariant; permutation is the orthogonal case, diagonal similarity is identical. With $r = (1 + \varepsilon_{\text{rel}})r_0$ and m, r_0 scaling by α , normalization is unchanged under $A \mapsto \alpha A$. \square

Lemma 9 (Hutchinson variance and SE-guard). *Let $B_k = T_k(\tilde{A})$ and $z \in \{\pm 1\}^n$ be i.i.d. Rademacher. Then $\mathbb{E}[z^\top B_k z] = \text{tr}(B_k)$ and $\text{Var}[z^\top B_k z] \leq 2\|B_k\|_F^2$. With p probes, the standard error satisfies $\text{se}_k \leq \sqrt{2}\|B_k\|_F/\sqrt{p}$ (scaled by $e^{-\eta k}$ for d_k). Consequently, the SE-guarded stopping rule $\hat{e}_k < \tau_e(1 + \gamma \text{relSE}_k)$ reduces false stops as p increases.*

Proposition 10 (Energy-tail guarantee). *Let $d_k = e^{-\eta k} \text{tr } T_k(\tilde{A})$ and $E_k = \sum_{j \leq k} d_j^2$. If $d_k^2/E_k < \tau$ holds for w consecutive steps from some index t onward and (d_k^2) is eventually nonincreasing, then*

$$\frac{\sum_{j>t} d_j^2}{E_t + \sum_{j>t} d_j^2} \leq \frac{\tau}{1 - \tau}.$$

Rank-sensitive corollary. Since $\|B_k\|_F \leq \sqrt{\text{rank}(B_k)}\|B_k\|_2$ and $\|B_k\|_2 \leq 1$ on $[-1, 1]$, one gets $p = \mathcal{O}(\text{rank}(B_k)\varepsilon^{-2} \log(1/\delta))$.

Corollary 11 (Uniform-in- k up to K). Fix $K \geq 1$ and $\delta \in (0, 1)$. With probability at least $1 - \delta$, for all $k = 0, 1, \dots, K - 1$,

$$|\hat{t}_k - \text{tr}(B_k)| \leq \|B_k\|_F \sqrt{\frac{2 \log(2K/\delta)}{p}}, \quad |\hat{s}_k - s_k| \leq e^{-\eta k} \|B_k\|_F \sqrt{\frac{2 \log(2K/\delta)}{p}}.$$

Proof. Apply Theorem 6 with $\delta \leftarrow \delta/K$ to each k and union bound over $k = 0, \dots, K - 1$. \square

A.2 Implementation Details

Spectral interval estimation. We estimate $(\lambda_{\min}, \lambda_{\max})$ via a few (3–5) steps of power and shifted-power iterations, optionally refined by Gershgorin disks; a small margin $\delta > 0$ is added. If the gap estimate is unstable, we fall back to a conservative spectral-radius bound.

Endpoint fallback (relative margin). If $(\lambda_{\min}, \lambda_{\max})$ estimation is unstable, we combine Gershgorin bounds with a few steps of (shifted) power iterations and then apply a *relative* safety margin $r = (1 + \varepsilon_{\text{rel}})r_0$. This keeps the scaling invariance intact even under $A \mapsto \alpha A$.

Stable numerics. We add $\varepsilon \in [10^{-12}, 10^{-10}]$ to denominators, cap condition numbers when forming small Hankels, and use randomized SVD if dense SVD is ill-conditioned. Chebyshev recurrences use the stable three-term update with periodic re-orthogonalization in mixed precision if needed.

Streaming memory. ASF-H stores only $(u_{k-1}^{(i)}, u_k^{(i)})$ per probe and streams probes in micro-batches, giving memory $\mathcal{O}(pn)$ (or $\mathcal{O}(n)$ with batching).

Stopping defaults and knobs. Recommended: $\eta = 0.06$, $K_{\min} = 2-3$, $K_{\max} = 64$, window $w = 2-3$, $\tau_e = 10^{-3}$ (retrieval) or 5×10^{-4} (fine discrimination), Hankel threshold $\tau_h = 10^{-3}$, Hutchinson $p = 64$ with Rademacher probes, SE-guard factor $\gamma = 2$.

Distance choices. Cosine on L2-normalized fingerprints is default. For heteroskedastic classes, a class-covariance-whitened (Mahalanobis) distance can improve separation; we also report Euclidean for ablations.

Views of a matrix. When A is not symmetric, use $H = \frac{1}{2}(A + A^\top)$ or $A^\top A$. Multiple views (e.g., adjacency, normalized Laplacian, kernel, covariance) can be concatenated or fused by late averaging.

A.3 Complexity Summary

Let Tmv denote the cost of a matrix–vector multiply with A .

- **CSF-K (exact traces).** Cost $\mathcal{O}(K \cdot \text{Tmv})$ for the Chebyshev recurrence plus one trace per order (via explicit trace only if diagonal known; otherwise use Hutchinson).
- **CSF-K (Hutchinson).** Cost $\mathcal{O}(pK \cdot \text{Tmv})$; trivially parallel across probes.
- **ASF (adaptive, exact).** As above with K replaced by $K^* \leq K_{\max}$ determined by the energy/Hankel stop.
- **ASF-H (adaptive, Hutchinson).** $\mathcal{O}(pK^* \cdot \text{Tmv})$, plus $\mathcal{O}(K^*)$ for Hankel/SVD on tiny ($\leq \lceil K^*/2 \rceil$) matrices.

A.4 Limitations and Extensions

Cospectral nonisomorphic graphs are indistinguishable to any trace-of-polynomial fingerprint. Combining multiple matrix views (e.g., adjacency and normalized Laplacian) or using joint fingerprints mitigates this in practice. For matrices with widely separated scales across tasks, per-task re-centering of η or per-coordinate whitening of ϕ can help.

B Appendix: Proofs

B.1 Auxiliary facts and references

We use (i) the telescoping identity $A^j - B^j = \sum_{i=0}^{j-1} A^{j-1-i}(A - B)B^i$, implying $\|A^j - B^j\|_2 \leq j \|A - B\|_2$ when $\|A\|_2, \|B\|_2 \leq 1$; (ii) $\|T_k(\tilde{A})\|_2 \leq \max_{x \in [-1, 1]} |T_k(x)| = 1$; (iii) Markov’s inequality on $[-1, 1]$: $\max_{x \in [-1, 1]} |p'(x)| \leq k^2 \max_{x \in [-1, 1]} |p(x)|$ for any degree- k polynomial p ; and the fact that for Chebyshev T_k , one can bound $\sum_{j=0}^k j |c_{k,j}| \leq C_T k^2$ with $C_T \leq 2$ (see, e.g., Rivlin, *Chebyshev Polynomials*, or standard coefficient/derivative bounds). For Hutchinson, we use the classical unbiasedness and variance bound for Rademacher probes.

B.2 Proof of Proposition 2

We write $\mathcal{N}(A)$ for the normalized matrix on which moments are computed. For symmetric (or symmetrized) inputs we use the affine normalization of Eq. (1):

$$\mathcal{N}(A) = \tilde{A} = \frac{A - m(A)I}{r(A)}, \quad m(A) = \frac{1}{2}(\lambda_{\max}(A) + \lambda_{\min}(A)), \quad r(A) = (1 + \varepsilon_{\text{rel}})\frac{1}{2}(\lambda_{\max}(A) - \lambda_{\min}(A)).$$

For markedly non-Hermitian inputs we use the radius fallback $\mathcal{N}(A) = A/R(A)$ with $R(A) = \max\{\rho(A), \varepsilon_{\text{rad}}\}$.

(a) Similarity, permutation, diagonal similarity. Let S be invertible, P a permutation (orthogonal), and D a positive diagonal. For any polynomial p one has

$$p(S^{-1}AS) = S^{-1}p(A)S,$$

hence $\text{tr } p(S^{-1}AS) = \text{tr } p(A)$ by cyclicity of trace.

Affine case. Similar matrices have the same eigenvalues, so $m(S^{-1}AS) = m(A)$ and $r(S^{-1}AS) = r(A)$. Therefore

$$\mathcal{N}(S^{-1}AS) = \frac{S^{-1}AS - m(A)I}{r(A)} = S^{-1} \left(\frac{A - m(A)I}{r(A)} \right) S = S^{-1}\mathcal{N}(A)S.$$

Since T_k is a polynomial, $T_k(\mathcal{N}(S^{-1}AS)) = S^{-1}T_k(\mathcal{N}(A))S$, and thus

$$s_k(S^{-1}AS) = \text{tr } T_k(\mathcal{N}(S^{-1}AS)) = \text{tr } S^{-1}T_k(\mathcal{N}(A))S = \text{tr } T_k(\mathcal{N}(A)) = s_k(A).$$

The cases $P^\top AP$ and $D^{-1}AD$ are particular instances of similarity.

Radius fallback. Spectral radius is similarity-invariant: $\rho(S^{-1}AS) = \rho(A)$, hence $R(S^{-1}AS) = R(A)$ and

$$\mathcal{N}(S^{-1}AS) = \frac{S^{-1}AS}{R(S^{-1}AS)} = S^{-1} \left(\frac{A}{R(A)} \right) S = S^{-1}\mathcal{N}(A)S.$$

The same trace-conjugation argument yields $s_k(S^{-1}AS) = s_k(A)$, and likewise for $P^\top AP$ and $D^{-1}AD$.

(b) Positive scaling $A \mapsto \alpha A$, $\alpha > 0$. *Affine case.* Eigenvalues scale: $\lambda_{\min}(\alpha A) = \alpha \lambda_{\min}(A)$ and $\lambda_{\max}(\alpha A) = \alpha \lambda_{\max}(A)$, so $m(\alpha A) = \alpha m(A)$, $r(\alpha A) = \alpha r(A)$, and therefore

$$\mathcal{N}(\alpha A) = \frac{\alpha A - \alpha m(A)I}{\alpha r(A)} = \frac{A - m(A)I}{r(A)} = \mathcal{N}(A).$$

Thus $s_k(\alpha A) = \text{tr } T_k(\mathcal{N}(\alpha A)) = \text{tr } T_k(\mathcal{N}(A)) = s_k(A)$.

Radius fallback. $\rho(\alpha A) = \alpha \rho(A)$ and hence $R(\alpha A) = \max\{\alpha \rho(A), \varepsilon_{\text{rad}}\}$. If $\rho(A) \geq \varepsilon_{\text{rad}}$ (the non-degenerate branch), then $R(\alpha A) = \alpha \rho(A)$ and

$$\mathcal{N}(\alpha A) = \frac{\alpha A}{\alpha \rho(A)} = \frac{A}{\rho(A)} = \mathcal{N}(A),$$

so moments are scale-invariant. If $\rho(A) = 0$ (the zero matrix), then $\mathcal{N}(A) = 0$ and $T_k(\mathcal{N}(A))$ is constant in A , so $s_k(\alpha A) = s_k(A)$ trivially.²

□

B.3 Proof of Proposition 10

Let t be the first index with $d_t^2/E_{t-1} < \tau$ and suppose d_t, \dots, d_{t+w-1} satisfy the rule. Then for $\ell \geq 0$,

$$d_{t+\ell}^2 \leq \tau E_{t+\ell-1} \leq \tau \left(E_t + \sum_{j=t+1}^{t+\ell-1} d_j^2 \right),$$

so the tail $\sum_{j>t} d_j^2$ is dominated by a geometric series with ratio at most τ , which gives $\sum_{j>t} d_j^2 \leq \frac{\tau}{1-\tau} E_t$. Returning the first index that satisfies the rule for w consecutive steps adds at most w to the stopping index. □

²If $0 < \rho(A) < \varepsilon_{\text{rad}}$, the ‘‘cap’’ $R(A) = \varepsilon_{\text{rad}}$ may break exact scale invariance; this regime is not used in our experiments and can be avoided by taking ε_{rad} sufficiently small.

B.4 Proof of Theorem 3

Recall $E_k = \sum_{j=0}^k s_j^2$, $e_k = s_k^2/(E_k + \varepsilon)$ and $r_k = \sigma_{\min}(H_k)/\sigma_{\max}(H_k)$. Algorithm 2 maintains a counter h and an indicator

$$\text{HIT}(k) \equiv (e_k < \tau_e \text{ or } r_k < \tau_h) \wedge (k+1 \geq K_{\min}),$$

updates $h \leftarrow h+1$ if $\text{HIT}(k)$ and $h \leftarrow 0$ otherwise, and returns at the first k with $h \geq w$ by setting $K^* \leftarrow k+1$.

Stopping index bound. Let $t \geq K_{\min} - 1$ be the smallest index such that $\text{HIT}(t), \text{HIT}(t+1), \dots, \text{HIT}(t+w-1)$ all hold; denote $k^* := t$. By the update rule, after processing $k = t+w-1$ we have $h = w$ and the algorithm returns with

$$K^* = (t+w-1) + 1 = t+w \leq k^* + w,$$

which proves the stated bound.

Tail-energy bound under the energy rule. Assume case (i) holds, i.e., the energy rule $e_k < \tau_e$ triggers w consecutive times starting at t . Suppose further that (s_k^2) is eventually nonincreasing (this standard regularity is the same as in Proposition 10). Because (s_k^2) is eventually nonincreasing, once s_k^2/E_k drops below τ_e it remains below τ_e for all subsequent indices.³ Hence there exists an index t (the same as above) such that $s_k^2/E_k < \tau_e$ for all $k \geq t$. Applying Proposition 10 with $\tau = \tau_e$ yields

$$\frac{\sum_{j>t} s_j^2}{E_t + \sum_{j>t} s_j^2} \leq \frac{\tau_e}{1 - \tau_e},$$

which is the claimed tail-energy control.

Remark on the stabilizer ε . Our implementation uses a tiny $\varepsilon > 0$ for numerical stability, i.e., $e_k = s_k^2/(E_k + \varepsilon)$. The proof above is exact for $\varepsilon = 0$; with $\varepsilon > 0$ the same bound holds after replacing τ_e by $\tau_e(1 + o(1))$ once $E_t \gg \varepsilon$, which is the regime of interest in all experiments. \square

B.5 Proof of Proposition 4

Write each real cosine mode as the real part of a complex exponential pair:

$$a_i \rho_i^k \cos(k\theta_i + \varphi_i) = \frac{1}{2} \left(c_i z_i^k + \overline{c_i z_i^k} \right), \quad z_i := \rho_i e^{i\theta_i}, \quad c_i := a_i e^{i\varphi_i}.$$

Let $u_k := \sum_{i=1}^r c_i z_i^k$ and note $s_k = \frac{1}{2}(u_k + \overline{u_k}) + \xi_k$. Consider the Hankel matrices $H_L(u) = [u_{i+j}]_{i,j=0}^{L-1}$ and $H_L(s) = [s_{i+j}]_{i,j=0}^{L-1}$.

Noiseless case ($\sigma = 0$). When $\xi_k \equiv 0$, the sequence u_k is a sum of at most r distinct exponentials. By classical Prony/Carathéodory–Fejér theory, u_k satisfies a linear recurrence of order at most r , which implies $\text{rank}(H_L(u)) \leq r$ for all L (e.g., $H_L(u)$ factors through Vandermonde/Krylov blocks built on $\{z_i\}_{i=1}^r$). Because $s_k = \frac{1}{2}(u_k + \overline{u_k})$, we have $H_L(s) = \frac{1}{2}(H_L(u) + \overline{H_L(u)})$, hence

$$\text{rank}(H_L(s)) \leq \text{rank}(H_L(u)) \leq r,$$

under the convention that one real cosine mode (a conjugate pair) counts as a single mode; if one counts conjugate exponentials separately, the bound becomes $\leq 2r$ (see Remark).

Noisy case ($\sigma > 0$). Let $H_L^{(0)} := H_L(s)$ in the noiseless case and write $H_L = H_L^{(0)} + N_L$, where N_L is the Hankel matrix formed by the noise sequence $\{\xi_k\}$: $(N_L)_{ij} = \xi_{i+j}$. For fixed L , standard norm inequalities yield $\|N_L\|_2 \leq C_L \sigma$ with a constant C_L depending only on L (e.g., by viewing N_L as a finite-dimensional linear map

³Formally, with $\varepsilon = 0$ one has $e_k = s_k^2/E_k$ and the ratio decreases whenever the numerator does not increase while the denominator does. With a tiny stabilizer $\varepsilon > 0$, the same conclusion holds up to an arbitrarily small slack; see the remark below.

from the coefficient vector $(\xi_0, \dots, \xi_{2L-2})$ to matrix entries and using $\|\cdot\|_2 \leq \|\cdot\|_F$. By Weyl's inequality for singular values,

$$\sigma_{r+1}(H_L) \leq \|N_L\|_2 \leq C_L \sigma, \quad \sigma_1(H_L) \geq \sigma_1(H_L^{(0)}) - \|N_L\|_2.$$

Since $\text{rank}(H_L^{(0)}) \leq r$, we have $\sigma_{r+1}(H_L^{(0)}) = 0$ and $\sigma_1(H_L^{(0)}) > 0$ unless the coefficients/pathological cancellations make the top singular value vanish.⁴ Hence, for any fixed L , as $\sigma \rightarrow 0$ one obtains

$$r_L = \frac{\sigma_{r+1}(H_L)}{\sigma_1(H_L)} \leq \frac{\|N_L\|_2}{\sigma_1(H_L^{(0)}) - \|N_L\|_2} \xrightarrow{\sigma \rightarrow 0} 0.$$

Therefore, for any $\tau_h > 0$ there exists $\sigma_0 > 0$ (depending on L, r and the mode parameters) such that if $\sigma < \sigma_0$ then $r_L < \tau_h$. \square

B.6 Lemma: Hutchinson moments (unbiasedness and SE bound)

Let B be fixed and $z \in \{\pm 1\}^n$ have i.i.d. Rademacher entries. Then $\mathbb{E}[z^\top Bz] = \text{tr}(B)$ and $\text{Var}(z^\top Bz) \leq 2\|B\|_F^2$. With p i.i.d. probes, the standard error satisfies $\text{se} \leq \sqrt{2}\|B\|_F/\sqrt{p}$.

B.7 Proof of Theorem 6

Unbiasedness (Hutchinson). Let $z \in \{\pm 1\}^n$ have i.i.d. Rademacher entries with $\mathbb{E}[zz^\top] = I$. Then for any (real) matrix B ,

$$\mathbb{E}[z^\top Bz] = \mathbb{E}\left[\sum_{i,j} z_i z_j B_{ij}\right] = \sum_i B_{ii} = \text{tr}(B).$$

Hence $\mathbb{E}[\widehat{t}_k] = \text{tr}(B_k)$ for $B_k = T_k(\widetilde{A})$, and $\mathbb{E}[\widehat{s}_k] = e^{-\eta k} \text{tr}(B_k) = s_k$.

Concentration for a single probe (Hanson–Wright). For z with i.i.d. Rademacher entries and any fixed real symmetric B , the Hanson–Wright inequality yields absolute constants $c_1, c_2 > 0$ such that

$$\Pr(|z^\top Bz - \text{tr}(B)| \geq t) \leq 2 \exp\left(-c_1 \min\left\{\frac{t^2}{\|B\|_F^2}, \frac{t}{\|B\|_2}\right\}\right).$$

In particular, since $\min\{x, y\} \geq x$ for all $x \leq y$, we have the looser but simpler bound

$$\Pr(|z^\top Bz - \text{tr}(B)| \geq t) \leq 2 \exp\left(-c_1 \frac{t^2}{\|B\|_F^2}\right).$$

Averaging p probes (sub-exponential Bernstein). Let $X_i = z^{(i)\top} B_k z^{(i)} - \text{tr}(B_k)$ (i.i.d. across i), and set $\overline{X} = \frac{1}{p} \sum_{i=1}^p X_i = \widehat{t}_k - \text{tr}(B_k)$. The tail bound above implies X_i are sub-exponential with Orlicz norm $\|X_i\|_{\psi_1} \leq C \|B_k\|_2$ and sub-Gaussian proxy $\|X_i\|_{\psi_2} \leq C \|B_k\|_F$ for an absolute $C > 0$. By the standard Bernstein inequality for sub-exponential variables, there exist absolute constants $c, C > 0$ such that for all $t > 0$,

$$\Pr(|\overline{X}| \geq t) \leq 2 \exp\left(-cp \min\left\{\frac{t^2}{\|B_k\|_F^2}, \frac{t}{\|B_k\|_2}\right\}\right).$$

Choose

$$t = \|B_k\|_F \sqrt{\frac{2 \log(2/\delta)}{cp}}$$

to get $\Pr(|\overline{X}| \geq t) \leq \delta$. Absorbing the (absolute) constant c into the numerical factor in the square root (redefining the leading “2” if desired), we obtain the displayed bound

$$|\widehat{t}_k - \text{tr}(B_k)| \leq \|B_k\|_F \sqrt{\frac{2 \log(2/\delta)}{p}} \quad \text{with probability at least } 1 - \delta.$$

⁴Generically $\sigma_1(H_L^{(0)}) > 0$ for any $L \geq 1$ if at least one mode has nonzero amplitude. If $\sigma_1(H_L^{(0)}) = 0$ for some finite L , one can increase L by a constant to avoid the degeneracy; this does not affect the argument.

From \widehat{t}_k to \widehat{s}_k and rank-sensitive form. Multiplying by $e^{-\eta k}$ yields

$$|\widehat{s}_k - s_k| = e^{-\eta k} |\widehat{t}_k - \text{tr}(B_k)| \leq e^{-\eta k} \|B_k\|_F \sqrt{\frac{2 \log(2/\delta)}{p}}.$$

Finally, for any matrix B_k , $\|B_k\|_F \leq \sqrt{\text{rank}(B_k)} \|B_k\|_2$. Since $B_k = T_k(\widetilde{A})$ and $\text{spec}(\widetilde{A}) \subset [-1, 1]$, we have $\|B_k\|_2 = \|T_k(\widetilde{A})\|_2 \leq \max_{x \in [-1, 1]} |T_k(x)| = 1$, giving the rank-sensitive variant

$$|\widehat{s}_k - s_k| \leq e^{-\eta k} \sqrt{\text{rank}(B_k)} \sqrt{\frac{2 \log(2/\delta)}{p}}.$$

□

B.8 Proof of Theorem 7

Write $T_k(x) = \sum_{j=0}^k c_{k,j} x^j$. Using the telescoping identity,

$$\|T_k(A) - T_k(B)\|_2 \leq \sum_{j=0}^k |c_{k,j}| \|A^j - B^j\|_2 \leq \sum_{j=0}^k |c_{k,j}| j \|A - B\|_2.$$

By a Markov-type coefficient bound for Chebyshev polynomials on $[-1, 1]$, $\sum_{j=0}^k j |c_{k,j}| \leq C_T k^2$ with $C_T \leq 2$ (see references above), hence

$$\|T_k(A) - T_k(B)\|_2 \leq C_T k^2 \|A - B\|_2.$$

Taking traces and using $|\text{tr}(M)| \leq n \|M\|_2$ yields

$$|\text{tr } T_k(A) - \text{tr } T_k(B)| \leq n C_T k^2 \|A - B\|_2.$$

With damping and normalization,

$$\begin{aligned} \|\phi_K(A) - \phi_K(B)\|_2 &\leq \frac{\left(\sum_{k=0}^{K-1} e^{-2\eta k} |\text{tr } T_k(A) - \text{tr } T_k(B)|^2 \right)^{1/2}}{\|\mathbf{s}_K(A)\|_2} \\ &\leq \frac{n}{\|\mathbf{s}_K(A)\|_2} \left(\sum_{k=0}^{K-1} e^{-2\eta k} C_T^2 k^4 \right)^{1/2} \|A - B\|_2. \end{aligned}$$

Since $\sum_{k \geq 0} e^{-2\eta k} k^4 = \Theta(\eta^{-5})$, the right-hand side is $\mathcal{O}(n \eta^{-5/2} \|A - B\|_2)$. Replacing A, B by $\widetilde{A}, \widetilde{B}$ gives the statement. □